Supplementary Information

Long-Lived Species Enhance Summertime Attribution of North American Ozone to Upwind Sources

Yixin Guo[†,‡,§], Junfeng Liu[*,†], Denise L. Mauzerall[‡,∥], Xiaoyuan Li[∥],

Larry W. Horowitz[⊥], Wei Tao[†] and Shu Tao[†]

[†]Laboratory of Surface Processes, College of Urban and Environmental Sciences, Peking University, Beijing, 100871, China

[‡]Woodrow Wilson School of Public and International Affairs, Princeton University, New Jersey, 08540, United States

[§]School of Physics, Peking University, Beijing, 100871, China

[∥]Department of Civil and Environmental Engineering, Princeton University, New Jersey, 08540, United States

[⊥]NOAA Geophysical Fluid Dynamics Laboratory, New Jersey, 08540-6649, United States

*Corresponding author: phone and fax: +86 10 6275 7852, email: jfliu@pku.edu.cn

The authors declare no competing financial interest.

The supporting information contains 22 pages, 10 figures and 7 tables.

List of Figures

S1. Relative difference of the sum of the tagged O_3 tracers to the standard O_3 (i.e., (O_3_EA + O_3_ELSE – O_3)/O_3) for the year 2000. Monthly data are presented and number is in percentage (%).

S2. Simulated (red lines) versus observed (blue dots) monthly mean concentrations of O_3 (ppbv) at surface and mountain sites over East Asia for the year 2000. Observational sites include Mt. Waliguan (China), Yonagunijima, Ryori, Minamitorishima, Tappi, Ogasawara, Sado-seki, Happo,Oki, Hedo (Japan).

S3. Definition of East Asia (EA: 15°N-50°N and 95°E-160°E) and its downwind receptor region North America (NA: 15°N-55°N and 60°W-125°W). The black dots denote the locations of observational sites where monthly surface O_3 observations for the year 2000 are compared with model results.

S4. Vertical-zonal cross-sections of the EA O_3 outflow (in ppbv) over the north Pacific (95°E-60°W, surface-200 hPa) at specified latitudes, using sensitivity analysis (removing EA_AE, left), NO_y-tagging (tagging NO_x, middle), and fully-tagged methods (tagging CO, VOCs and NO_x, right), in the summer of 2000. The solid bars help divide the entire region into East Asia, the Pacific and North America.

S5. Comparison of the labeling of selected O_3 precursor emissions and resulting products in NO_y-tagging (EA in red; East Asia anthropogenic emissions) and fully-tagged (EA and ELSE in orange; East Asia anthropogenic emissions and other emissions worldwide) mechanisms.

S6. longitudinal-vertical cross-sections of EA O_3 concentrations (ppbv, left column) and the production rates of EA O_3 ($10^{-15}\mathrm{molecules}/(\mathrm{s}\cdot\mathrm{cm}^3)$, right column) over the north Pacific and North America regions (95°E-60°W, from surface to 200 hPa) at specified latitudes (i.e., 20°N, 30°N, 40°N and 50°N) using the fully-tagged method in the summer of 2000.

S7. Attribution of seasonal mean surface O_3 concentrations to the anthropogenic O_3 precursors (all (first column), NO_x (second column) and VOCs plus CO (third column)) emissions from EA in different seasons.

S8. Estimated distribution of springtime surface ozone concentrations (ppbv) originating from EA (EA O_3) using sensitivity analysis (removal of East Asian anthropogenic emissions (EA_AE), top), NO_y-tagging (tagging EA_AE of NO_x, middle) and fully-tagged (tagging all EA_AE of ozone precursors including CO, VOCs, and NO_x, bottom) approaches. Arrows indicate wind velocity ($m \cdot sec^{-1}$).

S9. Vertical-zonal cross-sections of the ozone outflow (in ppbv) originating from EA_AE over the north Pacific (95 °E-60°W, surface-200 hPa), using a sensitivity analysis (removing EA_AE, left), tagged-NO_y species (tagging NO_x, middle), and fully-tagged method (tagging CO, VOCs and NO_x species, right) at specified latitudes, in the spring of 2000.

S10. Annual total, respiratory and cardiovascular mortality over North America (Unit mortalities/(year $\cdot 10^6$ km^2)) associated with acute exposure to transpacific transport of O_3 pollution using sensitivity analysis (first column), NO_y-tagging (second column) and fully-tagged (third column) in 2000, assuming no low concentration threshold

List of Tables

S1. Comparison of the influence of East Asian anthropogenic emissions (EA_AE) to the ground-level O_3 concentrations (ppbv) over North America (NA) from various studies

S2. Representative tagged emissions (CO, NO and VOCs) and tagged reservoir species (NO_y, RO_x and HO_x) in the fully-tagged method in MOZART-4.

S3. Representative photolysis reactions for the fully-tagged species

S4. Representative gas phase reactions for tagged species

S5. Comparison of the labeling of selected O_3 precursor emissions and resulting products in NO_y-tagging (EA in red; East Asia anthropogenic emissions) and fully-tagged (EA and ELSE in orange; East Asia anthropogenic emissions and other emissions worldwide) mechanisms.

S6. The 28 sigma levels of the NCEP reanalysis data

S7. Comparison of net ozone production and loss reaction amounts in the North American boundary layer (surface-800 hPa) attributable to East Asian anthropogenic emissions (EA_AE) by sensitivity, NO_y-tagging and fully-tagged approaches (unit: 10^{-15}molecules/(s · cm^3)), in summer and spring (in brackets) of 2000. $ISOPO_2$ is short for $HOCH_2COOCH_3CHCH_2$ and MPAN is short for $CH_2CCH_3CO_3NO_2$.

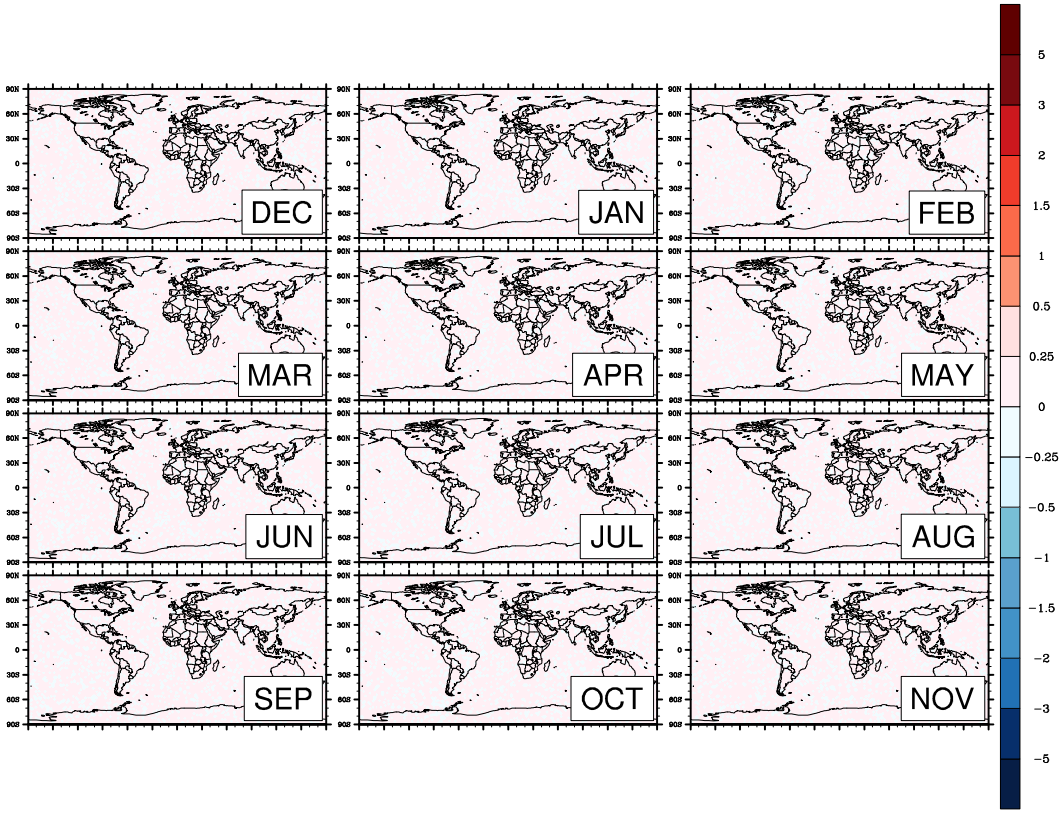

Figure S1 Relative difference of the sum of the tagged O_3 tracers to the standard O_3 (i.e., (O_3_EA + O_3_ELSE – O_3)/O_3) for the year 2000. Monthly data are presented and number is in percentage (%).

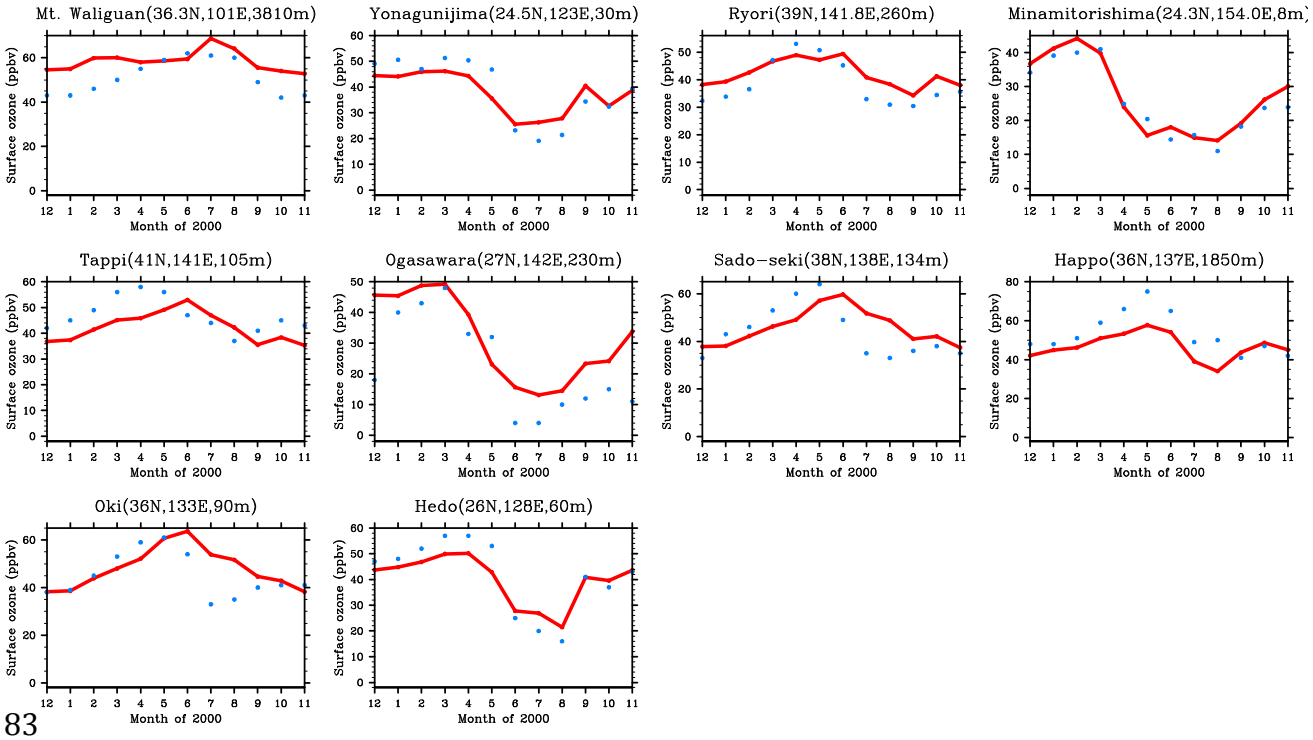

83

84 **Figure S2** Simulated (red lines) versus observed (blue dots) monthly mean concentrations of
85 O_3 (ppbv) at surface and mountain sites over East Asia for the year 2000. Observational sites
86 include Mt. Waliguan (China), Yonagunijima, Ryori, Minamitorishima, Tappi, Ogasawara,
87 Sado-seki, Happo,Oki, Hedo (Japan).

88

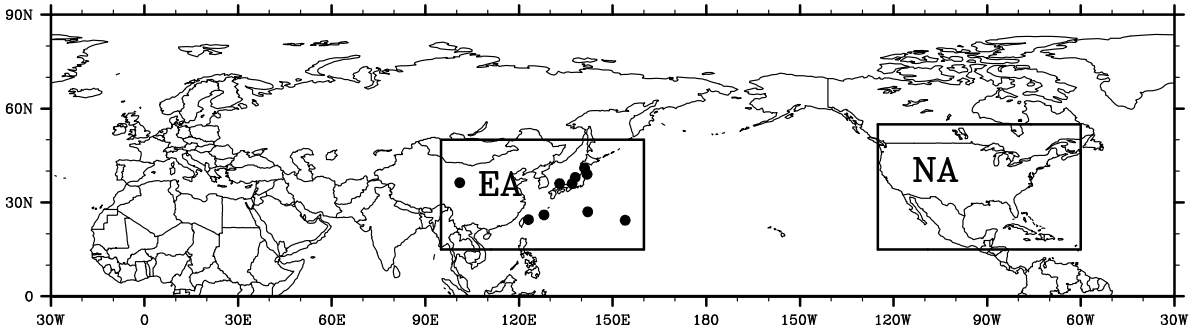

89

90 **Figure S3** Definition of East Asia (EA: 15°N-50°N and 95°E-160°E) and its downwind
91 receptor region North America (NA: 15°N-55°N and 60°W-125°W). The black dots denote the
92 locations of observational sites where monthly surface O_3 observations for the year 2000 are
93 compared with model results.

94

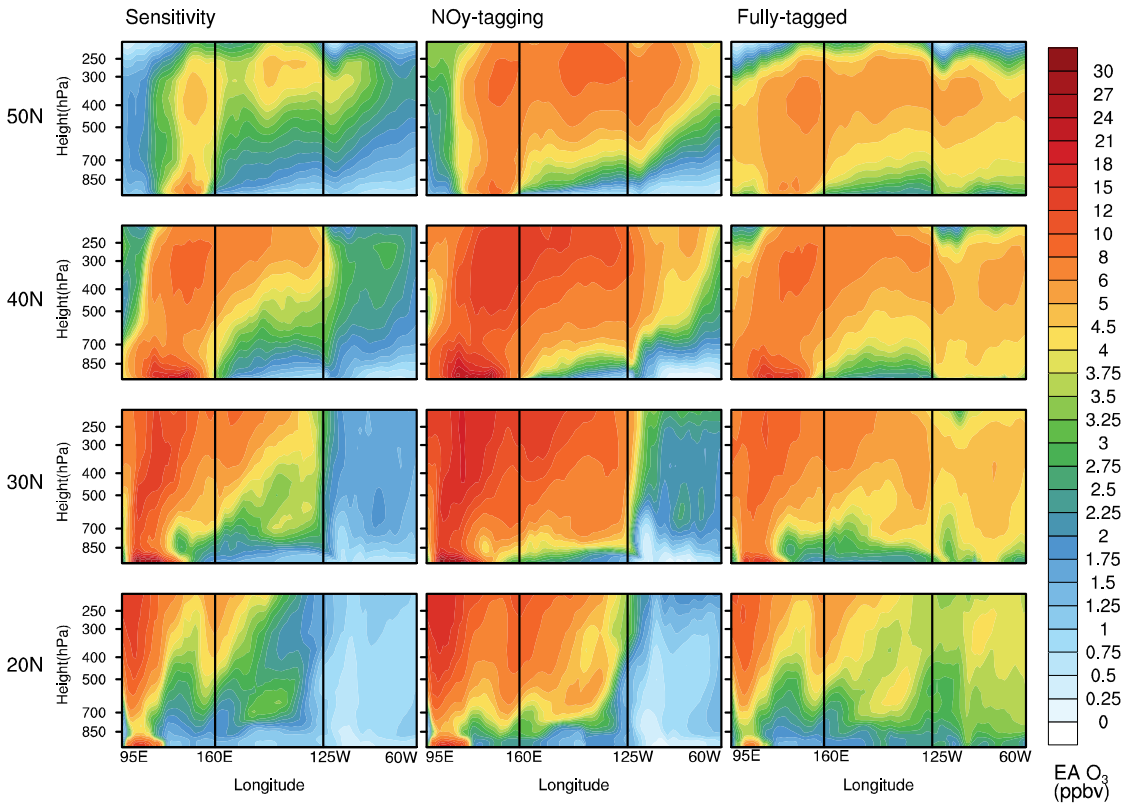

Figure S4 Vertical-zonal cross-sections of the EA O_3 outflow (in ppbv) over the north Pacific (95°E-60°W, surface-200 hPa) at specified latitudes, using sensitivity analysis (removing EA_AE, left), NO_y-tagging (tagging NO_x, middle), and fully-tagged methods (tagging CO, VOCs and NO_x, right), in the summer of 2000. The solid bars help divide the entire region into East Asia, the Pacific and North America.

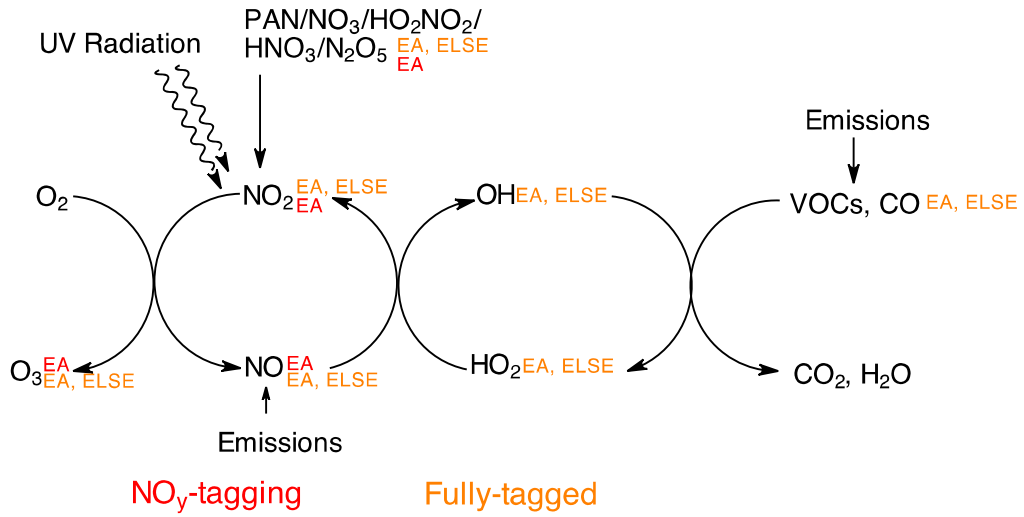

Figure S5 Comparison of the labeling of selected O_3 precursor emissions and resulting products in NO_y-tagging (EA in red; East Asia anthropogenic emissions) and fully-tagged (EA and ELSE in orange; East Asia anthropogenic emissions and other emissions worldwide) mechanisms.

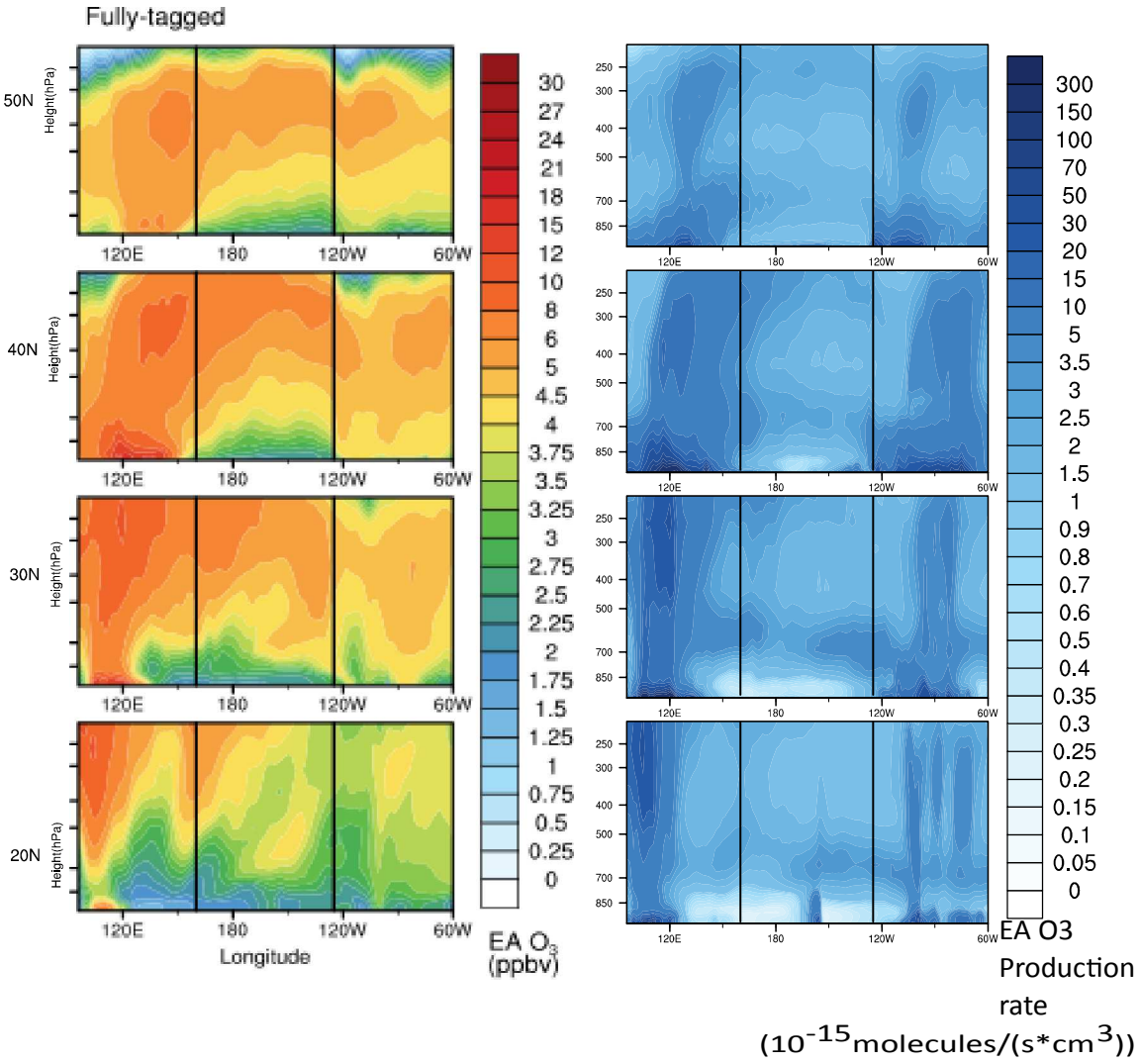

Figure S6 Longitudinal-vertical cross-sections of EA O_3 concentrations (ppbv, left column) and the production rates of EA O_3 (10^{-15}molecules/(s · cm^3), right column) over the north Pacific and North America regions (95°E-60°W, from surface to 200 hPa) at specified latitudes (i.e., 20°N, 30°N, 40°N and 50°N) using the fully-tagged method in the summer of 2000.

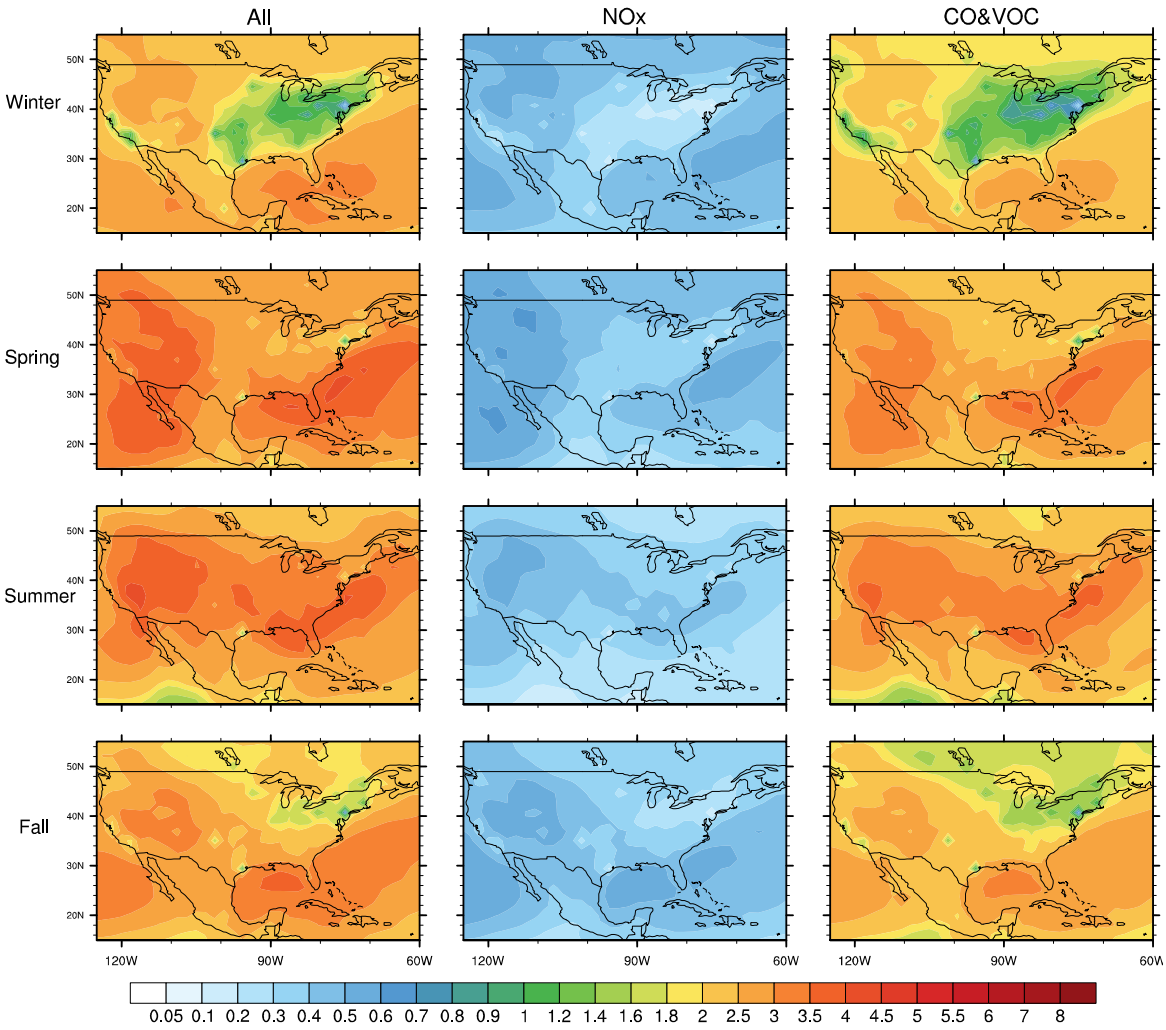

Figure S7 Attribution of seasonal mean surface O_3 concentrations to the anthropogenic O_3 precursors (all (first column), NO_x (second column) and VOCs plus CO (third column)) emissions from EA in different seasons.

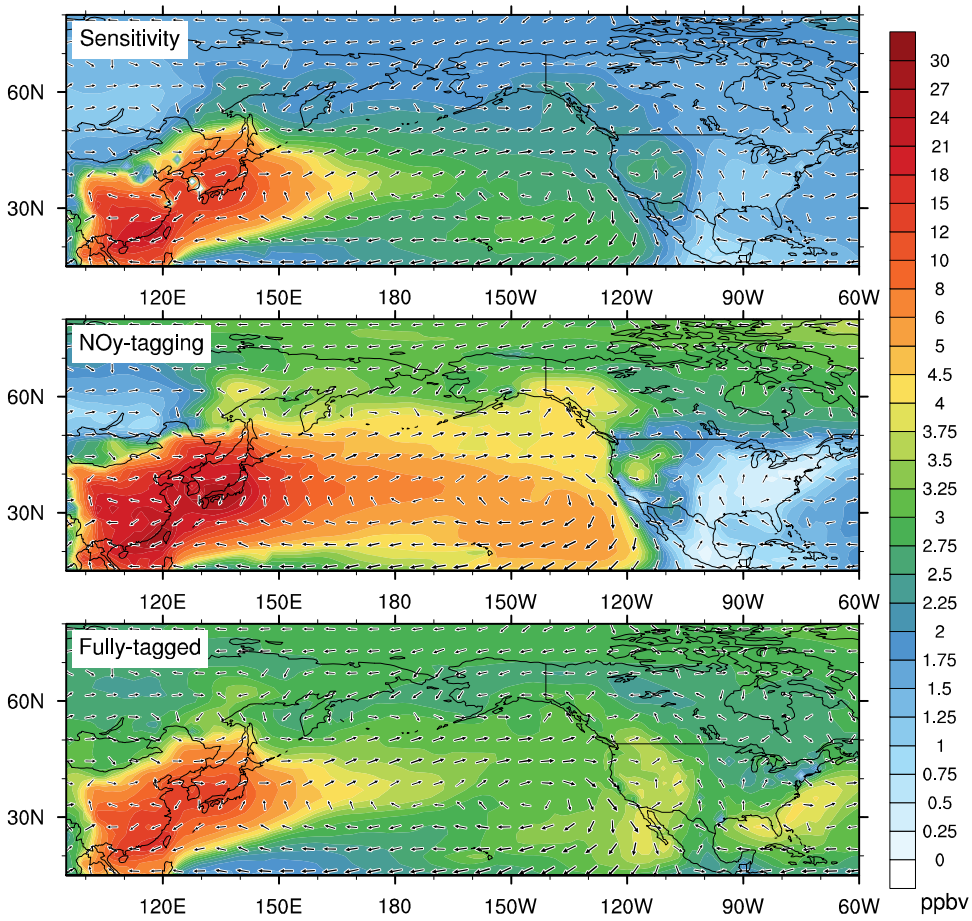

122

123 **Figure S8** Estimated distribution of springtime surface ozone concentrations (ppbv)
124 originating from EA (EA O_3) using sensitivity analysis (removal of East Asian anthropogenic
125 emissions (EA_AE), top), NO_y-tagging (tagging EA_AE of NO_x, middle) and fully-tagged
126 (tagging all EA_AE of ozone precursors including CO, VOCs, and NO_x, bottom) approaches.
127 Arrows indicate wind velocity ($m \cdot sec^{-1}$).

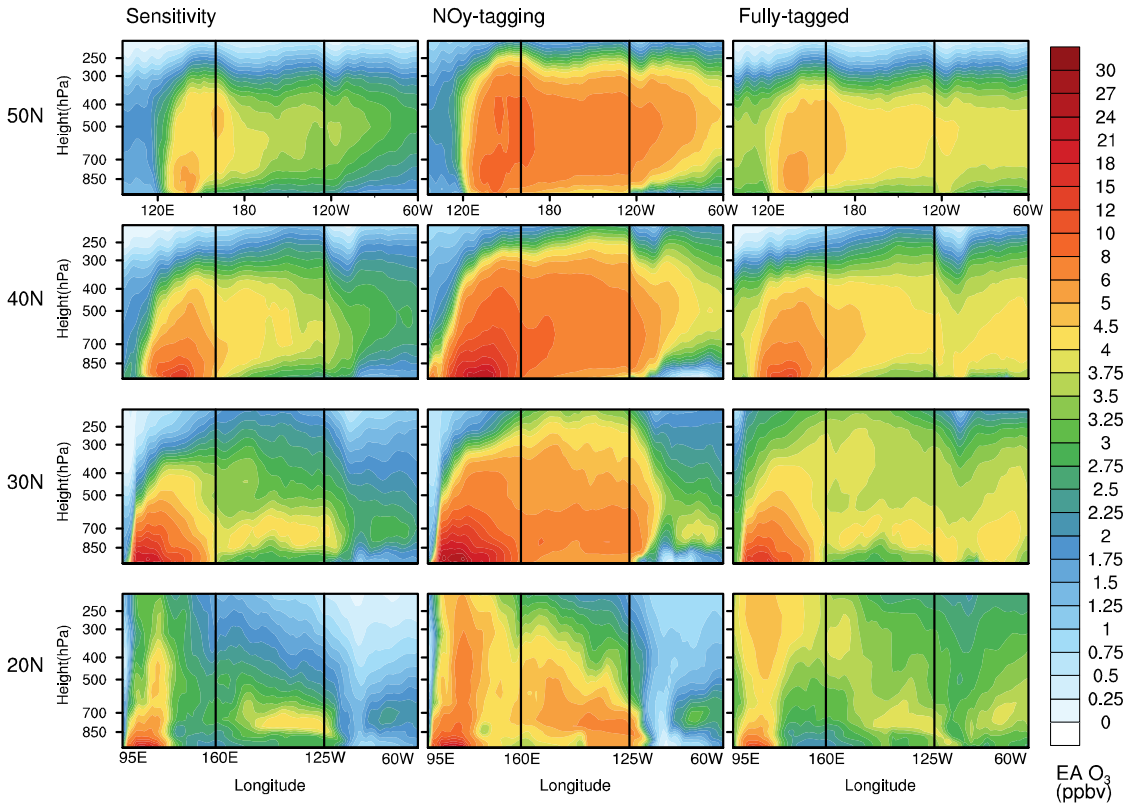

128

129 **Figure S9** Vertical-zonal cross-sections of the ozone outflow (in ppbv) originating from
130 EA_AE over the north Pacific (95 °E-60°W, surface-200 hPa), using a sensitivity analysis
131 (removing EA_AE, left), tagged-NO_y species (tagging NO_x, middle), and fully-tagged method
132 (tagging CO, VOCs and NO_x species, right) at specified latitudes, in the spring of 2000.

133

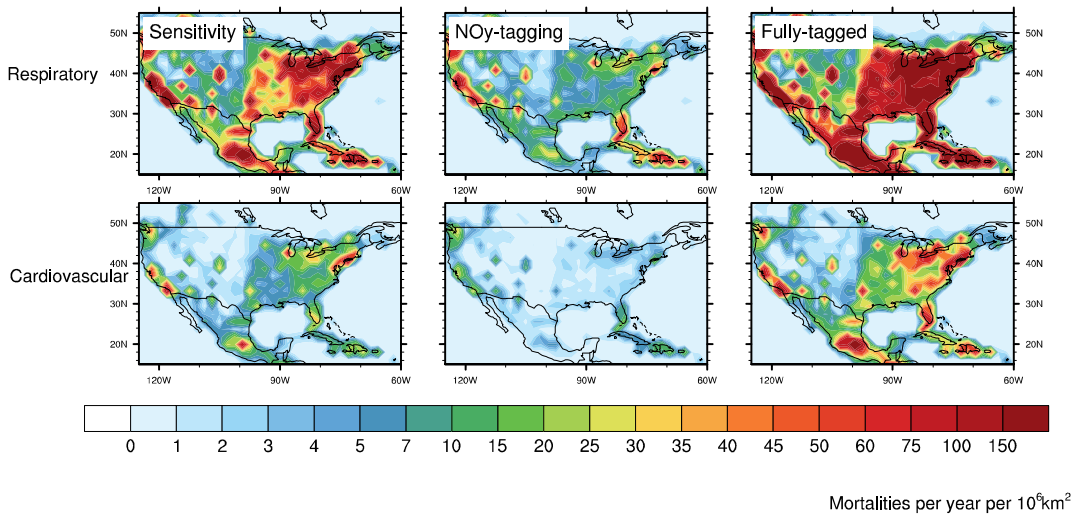

Figure S10 Annual total, respiratory and cardiovascular mortality over North America (Unit mortalities/(year ·10^6 km^2)) associated with acute exposure to transpacific transport of O_3 pollution using sensitivity analysis (first column), NO_y-tagging (second column) and fully-tagged (third column) in 2000, assuming no low concentration threshold.

147 **Table S1** Comparison of the influence of East Asian anthropogenic emissions (EA_AE) to the
148 ground-level O_3 concentrations (ppbv) over North America (NA) from various studies

Reference	Method	DJF	MAM	JJA	SON	Annual
Dentener, et al. [1] Table 4.2	Sensitivity study (NA Surface O_3 change due to a 20% decrease in EA_AE NO_x (multiplied by 5))	0.82	0.99	0.48	0.69	0.75
Fiore et al[2] SI	Sensitivity study (NA Surface O_3 change due to a 20% decrease in all EA_AE O_3 precursors (multiplied by 5))	1.30	1.45	0.67	0.88	1.08
Brown-Steiner et al.[3] Table 3	NO_y-tagging method (Contribution from all EA_AE O_3 precursors to NA surface O_3, Mean±interannual variability during 2001-2005)	2.29±0.41	2.35±0.56	0.70±0.31	1.19±0.53	1.63±0.45
This study	Sensitivity study (Change of NA surface O_3 due to 100% elimination of EA_AE O_3 precursors)	1.09	1.65	0.70	1.01	1.11
	NO_y-tagging method (Contribution from EA_AE NO_x to NA surface O_3)	1.20	1.62	0.52	0.83	1.04
	Fully-tagged method (Contribution from all EA_AE ozone precursors to NA surface O_3)	2.37	3.10	2.93	2.61	2.75

149

150

Table S2 Representative tagged emissions (CO, NO and VOCs) and tagged reservoir species (NO_y, RO_x and HO_x) in the fully-tagged method in MOZART-4.

Symbiotic name	Symbiotic name	Atomic composition
CO_EA	CO_ELSE	CO
NO_EA	NO_ELSE	NO
NO_2_EA	NO_2_ELSE	NO_2
C_2H_6_EA	C_2H_6_ELSE	C_2H_6
C_3H_6_EA	C_3H_6_ELSE	C_3H_6
C_3H_8_EA	C_3H_8_ELSE	C_3H_8
O_3_EA	O_3_ELSE	O_3
O1D_EA	O1D_ELSE	O1D
NO_3_EA	NO_3_ELSE	NO_3
HNO_3_EA	HNO_3_ELSE	HNO_3
HO_2NO_2_EA	HO_2NO_2_ELSE	HO_2NO_2
N_2O_5_EA	N_2O_5_ELSE	N_2O_5
OH_EA	OH_ELSE	OH
HO_2_EA	HO_2_ELSE	HO_2
H_2O_2_EA	H_2O_2_ELSE	H_2O_2
CO_EA	CO_ELSE	CO
$C_2H_5O_2$_EA	$C_2H_5O_2$_ELSE	$C_2H_5O_2$
CH_3O_2_EA	CH_3O_2_ELSE	CH_3O_2
CH_3OOH_EA	CH_3OOH_ELSE	CH_3OOH

Table S3 Representative photolysis reactions for the fully-tagged species

Original reaction	Tagged reactions
$O_3 + hv \rightarrow O1D + O_2$	$O_3\_EA + hv \rightarrow O1D\_EA + O_2$
	$O_3\_ELSE + hv \rightarrow O1D\_ELSE + O_2$
$NO_2 + hv \rightarrow NO + O$	$NO_2\_EA + hv \rightarrow NO\_EA + O\_EA$
	$NO_2\_ELSE + hv \rightarrow NO\_ELSE + O\_ELSE$
$N_2O_5 + hv \rightarrow NO_2 + NO_3$	$N_2O_5\_EA + hv \rightarrow NO_2\_EA + NO_3\_EA$
	$N_2O_5\_ELSE + hv \rightarrow NO_2\_ELSE + NO_3\_ELSE$

Table S4 Representative gas phase reactions for tagged species

Original reaction	Tagged reactions
$HO_2 + O_3 \rightarrow OH + 2O_2$	$HO_2\_EA + O_3\_EA \rightarrow OH\_EA$
	$HO_2\_ELSE + O_3\_ELSE \rightarrow OH\_ELSE$
	$HO_2\_EA + O_3\_ELSE \rightarrow .5*OH\_EA + .5*OH\_ELSE$
	$HO_2\_ELSE + O_3\_EA \rightarrow .5*OH\_EA + .5*OH\_ELSE$
$CO + OH \rightarrow CO_2 + HO_2$	$CO\_EA + OH\_EA \rightarrow HO_2\_EA$
	$CO\_ELSE + OH\_ELSE \rightarrow HO_2\_ELSE$
	$CO\_EA + OH\_ELSE \rightarrow 0.5*HO_2\_EA + 0.5*HO_2\_ELSE$
	$CO\_ELESE + OH\_EA \rightarrow 0.5*HO_2\_EA + 0.5*HO_2\_ELSE$
$NO + HO_2 \rightarrow NO_2 + OH$	$NO\_EA + HO_2\_EA \rightarrow NO_2\_EA + OH\_EA$
	$NO\_ELSE + HO_2\_ELSE \rightarrow NO_2\_ELSE + OH\_ELSE$
	$NO\_EA + HO_2\_ELSE \rightarrow 0.5*NO_2\_EA + 0.5*OH\_EA$ $+0.5*NO_2\_ELSE + 0.5*OH\_ELSE$
	$NO\_ELSE + HO_2\_EA \rightarrow 0.5*NO_2\_EA + 0.5*OH\_EA$ $+0.5*NO_2\_ELSE + 0.5*OH\_ELSE$

Special treatment of CH_4 in the fully-tagged method

In the standard MOZART-4 chemistry, CH_4 is simulated differently to other short-lived species such as CO and NO. There is no emissions for CH_4 and its concentration is 'fixed' in the upper and lower boundaries. The fully-tagged procedure doesn't tag CH_4 but does tag its oxidation products. For a chemical reaction that consumes or produces CH_4, the tagged reaction doesn't consume or generate additional CH_4 yet only records the evolvement of other tagged species. For example, in the tagged reactions of $CH_4 + OH \rightarrow CH_3O_2 + H_2O$, only the source of OH is discriminated and the tag follows the transformation from OH into CH_3O_2. CH_4 is not consumed by the tagged OH since it has been chemically consumed in the standard reaction.

Table S5 Tagging CH_4 in fully-tagged method.

Original reaction	Tagged reactions
$CH_4 + OH \rightarrow CH_3O_2 + H_2O$	$CH_4 + OH\_EA \rightarrow CH_3O_2\_EA + CH_4$ $CH_4 + OH\_ELSE \rightarrow CH_3O_2\_ELSE + CH_4$
$CH_4 + O1D \rightarrow 0.75*CH_3O_2 +$ $0.75*OH+0.25CH_2O+0.4*HO_2 + 0.05*H_2$	$CH_4 + O1D\_EA \rightarrow CH_4 + 0.75*CH_3O_2\_EA +$ $0.75*OH\_EA+0.25CH_2O\_EA+0.4*HO_2\_EA$ $CH_4 + O1D\_ELSE \rightarrow CH_4 + 0.75*CH_3O_2\_ELSE +$ $0.75*OH\_ELSE+0.25CH_2O\_ELSE+0.4*HO_2\_ELSE$ $NO\_EA + HO_2\_EA \rightarrow NO2\_EA + OH\_EA$
$C_3H_6 + O_3 \rightarrow 0.54*CH_2O + 0.19*HO_2$ $+0.33*OH + 0.08*CH_4 + 0.56*CO$ $+0.5CH_3CHO +0.31*CH_3O_2 +0.25CH_3COOH$	$C_3H_6\_EA + O_3\_EA \rightarrow 0.54*CH_2O\_EA + 0.19*HO_2\_EA+0.33*OH\_EA+$ $0.56*CO\_EA+0.5CH_3CHO\_EA +0.31*CH_3O_2\_EA+0.25CH_3COOH\_EA$ $C_3H_6\_ELSE + O_3\_ELSE \rightarrow 0.54*CH_2O\_ELSE +$ $0.19*HO_2\_ELSE+0.33*OH\_ELSE+ 0.56*CO\_ELSE+0.5CH_3CHO\_ELSE$ $+0.31*CH_3O_2\_ELSE+0.25CH_3COOH\_ELSE$ $C_3H_6\_EA + O_3\_ELSE \rightarrow 0.27*CH_2O\_EA +$ $0.095*HO_2\_EA+0.165*OH\_EA+ 0.28*CO\_EA+0.25CH_3CHO\_EA$ $+0.155*CH_3O_2\_EA+0.125CH_3COOH\_EA+$ $0.27*CH_2O\_ELSE + 0.095*HO_2\_ELSE+0.165*OH\_ELSE+$ $0.28*CO\_ELSE+0.25CH_3CHO\_ELSE$

	+0.155*CH_3O_2_ELSE+0.125CH_3COOH_ELSE
	C_3H_6_ELSE + O_3_EA → 0.27*CH_2O_EA + 0.095*HO_2_EA+0.165*OH_EA+ 0.28*CO_EA+0.25CH_3CHO_EA +0.155*CH_3O_2_EA+0.125CH_3COOH_EA+ 0.27*CH_2O_ELSE + 0.095*HO_2_ELSE+0.165*OH_ELSE+ 0.28*CO_ELSE+0.25CH_3CHO_ELSE +0.155*CH_3O_2_ELSE+0.125CH_3COOH_ELSE

171

172

173 **Table S6** The 28 sigma levels of the NCEP reanalysis data

	Sigma levels
1	0.9950
2	0.9821
3	0.9644
4	0.9425
5	0.9159
6	0.8838
7	0.8458
8	0.8014
9	0.7508
10	0.6943
11	0.6329
12	0.5681
13	0.5017
14	0.4357
15	0.3720
16	0.3125
17	0.2582
18	0.2101

19	0.1682
20	0.1326
21	0.1028
22	0.0782
23	0.0580
24	0.0418
25	0.0288
26	0.0183
27	0.0101
28	0.0027

174

175

176 **Table S7** Comparison of net ozone production and loss reaction amounts in the North
177 American boundary layer (surface-800 hPa) attributable to East Asian anthropogenic emissions
178 (EA_AE) by sensitivity, NO_y-tagging and fully-tagged approaches (unit: 10^{-15}molecules/(s·
179 cm^3)), in summer and spring (in brackets) of 2000. $ISOPO_2$ is short for
180 $HOCH_2COOCH_3CHCH_2$ and MPAN is short for $CH_2CCH_3CO_3NO_2$.

Reaction amounts contributed by EA_AE averaged over NA boundary layer	Base	Sensitivity	NO_y-tagging	Fully-tagged
Production of NO_2				
HO_2+NO→OH+NO_2	91.90(66.90)	0.47(1.21)	0.23(0.66)	6.23(5.16)
RO_2+NO→RO+NO_2	77.23(47.42)	-0.28(-0.33)	0.18(0.45)	4.51(3.05)
CH_3O_2+NO→CH_2O+HO_2+NO_2	23.87(17.62)	-0.14(-0.26)	0.09(0.25)	1.67(1.33)
$ISOPO_2$+NO→R'O_2+HO_2+NO_2	18.30(7.04)	-0.06(-0.05)	0.03(0.03)	0.84(0.35)
CH_3CO_3+NO→CH_3O_2+CO_2+NO_2	11.09(7.48)	-0.01(0.01)	0.02(0.07)	0.68(0.50)
HO_2NO_2+$M/h\nu$ → HO_2+ NO_2	89.51(50.64)	1.07(1.62)	0.13(0.35)	5.16(3.40)
N_2O_5+$M/h\nu$ → NO_2+ NO_3	70.30(31.36)	1.17(1.27)	0.07(0.26)	3.41(1.79)

$NO_3+h\nu \rightarrow .89*NO_2 + .11*NO + .93*O_3$	2.79(1.80)	0.06(0.09)	0.01(0.03)	0.19(0.13)
$HNO_3+h\nu \rightarrow OH + NO_2$	0.10(0.09)	0.01(0.01)	0.0006(0.002)	0.02(0.02)
PAN+hv/M→ NO_2+ CH_3CO_3	46.50(24.75)	0.37(0.74)	0.08(0.27)	2.62(1.57)
MPAN+hv/M→ NO_2	15.32(4.59)	0.09(0.07)	0.82(0.27)	0.01(0.01)
Loss of NO_2				
NO_2+hv→ NO + O	811(809.10)	4.89(6.89)	1.72(5.74)	50.89(51.96)
Loss of O_3				
$O_3+H_2O \rightarrow OH+2O_2$	37.91(25.94)	0.06(0.84)	0.54(0.93)	2.85(1.99)
$O_3+OH \rightarrow HO_2+O_2$	5.42(4.32)	0.06(0.04)	0.08(0.16)	0.42(0.34)
$O_3+HO_2 \rightarrow OH+2O_2$	18.76(13.00)	0.48(0.78)	0.29(0.55)	1.43(1.02)
$C_2H_4/C_3H_6/C_5H_8/CH_2CHCOCH_3/CH_2CCH_3CHO+O_3 \rightarrow RO$	4.48(1.39)	0.05(0.04)	0.005(0.003)	0.32(0.01)
O_3+ C_5H_8	2.85(0.70)	0.03(0.02)	0.03(0.02)	0.2(0.05)

References:

1. Dentener, F.; Keating, T.; Akimoto, H. HTAP (hemispheric transport of air pollution)(2010): part A: ozone and particulate matter air pollution studies Nr. 17. *United Nations Publication, New York* **2011**,

2. Fiore, A. M.; Dentener, F. J.; Wild, O.; Cuvelier, C.; Schultz, M. G.; Hess, P.; Textor, C.; Schulz, M.; Doherty, R. M.; Horowitz, L. W.; MacKenzie, I. A.; Sanderson, M. G.; Shindell, D. T.; Stevenson, D. S.; Szopa, S.; Van Dingenen, R.; Zeng, G.; Atherton, C.; Bergmann, D.; Bey, I.; Carmichael, G.; Collins, W. J.; Duncan, B. N.; Faluvegi, G.; Folberth, G.; Gauss, M.; Gong, S.; Hauglustaine, D.; Holloway, T.; Isaksen, I. S. A.; Jacob, D. J.; Jonson, J. E.; Kaminski, J. W.; Keating, T. J.; Lupu, A.; Marmer, E.; Montanaro, V.; Park, R. J.; Pitari, G.; Pringle, K. J.; Pyle, J. A.; Schroeder, S.; Vivanco, M. G.; Wind, P.; Wojcik, G.; Wu, S.; Zuber, A. Multimodel estimates of intercontinental source-receptor relationships for ozone pollution. *J. Geophys. Res., [Atmos.]* **2009,** *114*; DOI10.1029/2008jd010816

197 3. Brown-Steiner, B.; Hess, P. Asian influence on surface ozone in the United States: A
198 comparison of chemistry, seasonality, and transport mechanisms. *J. Geophys. Res.,*
199 *[Atmos.]* **2011,** *116*; DOI10.1029/2011JD015846

200